Auxiliary field Monte Carlo for charged particles

A. C. Maggs
Laboratoire de Physico-Chimie Théorique, UMR CNRS-ESPCI 7083, 10 Rue Vauquelin, F-75231 Paris Cedex 05, France

(Received 25 August 2003; accepted 20 November 2003)

This article describes Monte Carlo algorithms for charged systems using constrained updates for the electric field. The method is generalized to treat inhomogeneous dielectric media, electrolytes via the Poisson–Boltzmann equation and considers the problem of charge and current interpolation for off lattice models. We emphasize the differences between this algorithm and methods based on the electrostatic potential, calculated from the Poisson equation. © *2004 American Institute of Physics.* [DOI: 10.1063/1.1642587]

I. INTRODUCTION

Fast methods for calculating Coulomb interactions are of the greatest importance in the simulation of charged condensed matter systems. Several algorithms are available including multipole[1] and Fourier based[2] methods; they permit efficient molecular dynamics simulations but are ill-adapted to Monte Carlo simulation. These methods have been widely used and implemented; recent research has led to multi-time step algorithms and aims at generalizing the methods to multiprocessor environments. Despite this effort the Coulomb loop is still the slowest part of many simulation codes[3].

An alternative approach, the subject of this paper, is to use an auxiliary field in order to calculate the Coulomb interaction in a manner familiar from electromagnetism. Many books[4,5] consider the following scalar functional:

$$\mathcal{F}(\phi)=\int\left[\frac{\epsilon_0}{2}(\text{grad}\,\phi)^2-\rho\phi\right]\mathrm{d}^3\mathbf{r}, \tag{1}$$

where ρ is the charge density imposed by the experimental geometry and ϕ is a freely variable field. One might hope that one could use this functional to construct alternative, and more efficient algorithms due to the *local* nature of the energy function. One is instructed to minimize Eq. (1) by taking the functional derivative with respect to ϕ; this leads to Poisson's equation familiar from electrostatics,

$$\nabla^2\phi_p=-\rho/\epsilon_0. \tag{2}$$

Thus we have a minimum principle; we can identify the function ϕ_p which minimizes Eq. (1) with the electrostatic potential. However when we substitute the solution of Eq. (2) in Eq. (1) (using appropriate boundary conditions) we find

$$\mathcal{F}(\phi_p)=-\int\frac{\epsilon_0}{2}(\text{grad}\,\phi_p)^2\mathrm{d}^3\mathbf{r}. \tag{3}$$

This is the *negative* of the true electrostatic energy. Recently[6] a series of such potential functionals have been introduced in order to treat inhomogeneous dielectric systems, such as interfaces and pores, however all the functionals have a similar sign defect.

This sign change is a major problem for numerical work. It implies that the same energy can not be used to evolve the field and the particle degrees of freedom in parallel. Clearly if one tries to do Monte Carlo with ϕ one generates the partition function

$$\mathcal{Z}(\rho)=\int\mathcal{D}\phi e^{-\beta\mathcal{F}(\phi)}=e^{-\beta\mathcal{F}(\phi_p)}\times\text{const} \tag{4}$$

as can be seen by substituting $\phi=\phi_p+\tilde{\phi}$. This is the wrong statistical weight for particles interacting via Coulomb's law. While evaluation of the energy *seems* to have been reduced to a local calculation in practice a *global* optimization is needed every time step to minimize Eq. (1) and then flip the sign of the result. For Monte Carlo this leads to such a level of inefficiency that the method is useless.

This sign problem is most surprising: We are aware that Maxwell's equations allow the co-evolution of field and particles with the correct sign of the electromagnetic energy. What has gone wrong in the formulation of electrostatics in terms of an auxiliary field? The solution to the paradox is found by recognizing that the correct sign of interaction is only possible with a *vector* field, a point made forcefully in Ref. 7 in a general discussion of the forces of nature.

II. VECTOR FUNCTIONALS

Recently,[8] an efficient Monte Carlo algorithm for charged systems was formulated using electric field lines (rather than the electrostatic potential) as the true dynamic degree of freedom. The algorithm consists of a local energy functional together with *local* update rules; no global optimization is needed. Coulomb interactions result from the energy

$$\mathcal{U}=\frac{\epsilon_0}{2}\int\mathbf{E}^2\,\mathrm{d}^3\mathbf{r}, \tag{5}$$

where the electric field, $\mathbf{E}$ is constrained by Gauss' law, $\text{div}\,\mathbf{E}-\rho/\epsilon_0=0$. Introduction of a Lagrange multiplier for the constraint implies that the minimum energy is indeed

$$\mathcal{U}_p(\phi_p)=\int\frac{\epsilon_0}{2}(\text{grad}\,\phi_p)^2\mathrm{d}^3\mathbf{r}, \tag{6}$$

with ϕ_p (now the Lagrange multiplier) again the solution to Poisson's equation.

We now show that the use of the energy Eq. (5) at finite temperature still leads to pure Coulomb interactions. Let us define a partial partition function by integrating over the electric field but *not* the particle positions, $\mathbf{r}_i$:

$$\mathcal{Z}(\mathbf{r}_i) = \int \mathcal{D}\mathbf{E} \prod_{\mathbf{r}} \delta(\operatorname{div}\mathbf{E} - \rho(\mathbf{r}_i)/\epsilon_0) e^{-\beta \mathcal{U}}. \tag{7}$$

Let us evaluate the integral by changing variables, $\mathbf{E}_{\mathrm{tr}} = \mathbf{E} + \operatorname{grad}\phi_p$. We find that

$$\begin{aligned}\mathcal{Z}(\mathbf{r}_i) &= \int \mathcal{D}\mathbf{E}_{\mathrm{tr}} \prod_{\mathbf{r}} \delta(\operatorname{div}\mathbf{E}_{\mathrm{tr}}) e^{-\beta(\epsilon_0/2)\int (\mathbf{E}_{\mathrm{tr}} - \operatorname{grad}\phi_p)^2 \mathrm{d}^3\mathbf{r}} \\ &= e^{-\beta(\epsilon_0/2)\int (\operatorname{grad}\phi_p)^2} \\ &\quad \times \int \mathcal{D}\mathbf{E}_{\mathrm{tr}} \prod_{\mathbf{r}} \delta(\operatorname{div}\mathbf{E}_{\mathrm{tr}}) e^{-\beta(\epsilon_0/2)\int \mathbf{E}_{\mathrm{tr}}^2 \mathrm{d}^3\mathbf{r}} \\ &= \mathcal{Z}_{\mathrm{Coulomb}}(\mathbf{r}_i) \times \mathrm{const.}\end{aligned} \tag{8}$$

The cross term in the energy, $\int \mathbf{E}_{\mathrm{tr}} \cdot \operatorname{grad}\phi_p \mathrm{d}^3\mathbf{r}$, is identically zero as can be seen by integration by parts. We discover that integration over the tranverse modes multiplies the statistical weight of each configuration by a constant. The longitudinal component of the electric field, $-\operatorname{grad}\phi_p$, produces an effective Coulomb interaction between the particles.

We shall now give a full description of the algorithm showing how configurations can be dynamically generated according to the constrained statistical weight in Eq. (7). This gives rise to a lattice gas in which charges are confined to a grid. We demonstrate numerically the efficiency of the algorithm for a system of lattice dipoles. A coarse graining of the electric degrees of freedom leads to a new algorithm for treating the Poisson–Boltzmann equation as well as a *nonconstrained* algorithm for the Yukawa potential. We then show how to treat off lattice models by interpolating charges to the grid. We show that the generalization of the algorithm to inhomogeneous dielectric media automatically resums a large class of fluctuation based potentials such as the Keesom potential, capturing important characteristics of polar dielectric materials which are missed by the Poisson equation.

III. PERIODIC BOUNDARY CONDITIONS

A. Conventional approach

Imposition of periodic boundary conditions in systems interacting with Coulomb interactions is subtle due to the conditional convergence of Coulomb sums:[9] When extrapolating periodic images of the system to infinity there is a residual dependency on the dielectric constant, ϵ_s of the surrounding medium.

The total potential, Φ is the sum of ϕ_p, coming from the solution of the Poisson equation with periodic boundary conditions, and a dipolar contribution: $\Phi = \phi_p + \phi_d$. Here,

$$\phi_d = -\overline{\mathbf{E}} \cdot \mathbf{r}, \tag{9}$$

where $\overline{\mathbf{E}}$ is a vector proportional to the dipole moment per unit volume of the simulation cell, $\mathbf{d}_E$,[9]

$$\overline{\mathbf{E}} = -\frac{1}{\epsilon_0(1+2\epsilon_s)} \mathbf{d}_E. \tag{10}$$

This constant field reminds us of the "depolarizing field" in elementary treatments of spherical dielectric media.[4] Two common choices of boundary condition are "tinfoil" with $\epsilon_s = \infty$ and "vacuum," $\epsilon_s = 1$. Clearly the tinfoil limit corresponds to keeping just the periodic potential, ϕ_p.

The field $\overline{\mathbf{E}}$ generates a purely additive contribution to the energy density,

$$u_0 = \frac{\mathbf{d}_E^2}{2\epsilon_0(1+2\epsilon_s)}. \tag{11}$$

This extra energy term can be awkward to handle in molecular dynamics; its definition leads to discontinuities in the energy function since $\mathbf{d}_E = (1/V)\Sigma_i e_i \mathbf{r}_i$ is calculated with a given, fixed Bravais lattice; V is the simulation volume, e_i the charge of particle i at position $\mathbf{r}_i$ in the simulation cell.

B. Constrained algorithm

The general solution to Gauss' law in periodic systems is

$$\mathbf{E} = -\operatorname{grad}\phi_p + \operatorname{curl}\mathbf{Q} + \overline{\mathbf{E}}, \tag{12}$$

where $\mathbf{E}_{\mathrm{tr}} = \operatorname{curl}\mathbf{Q}$ is an arbitrary transverse field. Our algorithm is closely related to the following Maxwell equation:[10]

$$\epsilon_0 \frac{\partial \mathbf{E}}{\partial t} = -\mathbf{J} + \operatorname{curl}\mathbf{H}, \tag{13}$$

with $\mathbf{J}$ the electric current and $\mathbf{H}$ the magnetic strength. If we start a simulation in a state in which $\overline{\mathbf{E}} = 0$, then an evolution of the field according to Eq. (13) (as well, it will be seen, as with our algorithm) generates fields with

$$\overline{\mathbf{E}}(t) = -\frac{1}{V}\int \mathrm{d}t \int \mathrm{d}^3\mathbf{r}\, \mathbf{J}/\epsilon_0 = -\mathbf{d}/\epsilon_0 \tag{14}$$

so defining $\mathbf{d}$. We have used the fact that the integral of the curl of a periodic function is zero. This is *very similar* to the Ewald convention of Eq. (10) with $\epsilon_s = 0$. We note that this choice is rather unconventional, one normally considers $1 < \epsilon_s < \infty$.

If the charges in the simulation are bound (so as to remain in the basic unit cell), then $\mathbf{d} = \mathbf{d}_E$. If there are free charges in the simulation, $\pm e$, then the same configuration can be produced by different currents which wind about the periodic system: We only require that $\mathbf{d} - \mathbf{d}_E = e\mathbf{b}/V$, where $\mathbf{b}$ is a Bravais lattice vector. We again find that there is an additive contribution to the energy density of the form

$$u_0 = \frac{\mathbf{d}^2}{2\epsilon_0}. \tag{15}$$

We note the natural use of $\mathbf{d}$ rather than $\mathbf{d}_E$ is a great advantage for molecular dynamic simulation. It leads to energies which are continuous functions of the particle position.

In our simulations of periodic systems we are also capable of reproducing tinfoil boundary conditions. We do this

by adding a constant electric field $\mathbf{E}_g$ to the zero wave vector component of the electric field, so that $\overline{\mathbf{E}} = -\mathbf{d}/\epsilon_0 + \mathbf{E}_g$. This leads to a simple modification of u_0,

$$u_0 = \frac{(\mathbf{d} - \epsilon_0 \mathbf{E}_g)^2}{2\epsilon_0}. \tag{16}$$

Integration over $\mathbf{E}_g$ as well as the transverse field now leads to an effective statistical weight which varies as $e^{-\beta/2\int(\mathrm{grad}\,\phi_p)^2 \mathrm{d}^3\mathbf{r}}$. The particles interact through the periodic solution to Poisson's equation, ϕ_p.

Finally in this section we note that a consistent description of polarization effects in quantum mechanics (based on considerations of gauge invarience) require the use of $\mathbf{d}$ rather than $\mathbf{d}_E$ for the polarization.[11]

IV. A SCALAR FUNCTIONAL VIA GAUGE TRANSFORMATIONS

In this section we continue the development of our formulation of the electrostatic potential in order to show that despite the failure of the variational principle Eq. (1) it is possible to link the electrostatic energy Eq. (5) to a scalar potential. This section is independent of the practical implementation of the algorithm and may be omitted on first reading.

Our separation of the electric field into longitudinal and transverse components is similar in many ways to the Coulomb gauge in conventional electromagnetism. It leads, however, to a description of the dynamics in terms of potentials which is nonlocal; as in conventional electromagnetism other choices of gauge are possible.

Let us write the electric field in an arbitrary gauge in the form

$$\mathbf{E} = -\,\mathrm{grad}\,\phi - \mathbf{A}. \tag{17}$$

From Gauss' law we deduce that $\rho/\epsilon_0 = -\nabla^2\phi - \mathrm{div}\,\mathbf{A}$. We now apply a gauge condition

$$\mathrm{div}\,\mathbf{A} + \alpha\frac{\partial\phi}{\partial t} = 0 \tag{18}$$

for some constant α. We discover that the propagation of the potential ϕ is now local

$$\alpha\frac{\partial\phi}{\partial t} = \nabla^2\phi + \rho/\epsilon_0. \tag{19}$$

The dynamics of the electric field in the algorithm are related to the Langevin equation[10]

$$\frac{\partial\mathbf{E}}{\partial t} = (\epsilon_0\nabla^2\mathbf{E} - \mathrm{grad}\,\rho)/\xi - \mathbf{J}/\epsilon_0 + \boldsymbol{\zeta}(t), \tag{20}$$

where ξ sets the time scale of the dynamics and $\boldsymbol{\zeta}(t)$ is a transverse noise. From these equations we see that the special choice $\epsilon_0\alpha = \xi$ allows a particularly simple equation for the vector potential $\mathbf{A}$,

$$\frac{\partial\mathbf{A}}{\partial t} = \frac{1}{\alpha}\nabla^2\mathbf{A} + \mathbf{J}/\epsilon_0 + \boldsymbol{\zeta}(t). \tag{21}$$

In this diffusive gauge we calculate the electric energy Eq. (5) in terms of the potentials

$$\mathcal{U} = \int\left\{\rho\phi - \frac{\epsilon_0}{2}(\mathrm{grad}\,\phi)^2 + \frac{\epsilon_0\mathbf{A}^2}{2}\right\}\mathrm{d}^3\mathbf{r}. \tag{22}$$

Cross terms in $\mathbf{A}\cdot\mathrm{grad}\,\phi$ have been eliminated with help of the gauge condition and by using the equation of motion for the scalar potential. We recognize that this functional is closely related to the naive scalar functional Eq. (1); it is, however, dynamically constrained by Eq. (18).

V. ALGORITHM

The Monte Carlo algorithm uses the Metropolis criterion together with the constrained energy function Eq. (5). In order to generate configurations according to the statistical weight of Eq. (7) we need to:

(a) Move particles without violating the constraint of Gauss' law to preserve the delta function on $\mathrm{div}\,\mathbf{E} - \rho/\epsilon_0$;
(b) Integrate over the transverse degrees of freedom $\mathbf{E}_{\mathrm{tr}}$, of the electric field;
(c) Integrate over $\mathbf{E}_g$.

Our third Monte Carlo step eliminates the slaving of $\overline{\mathbf{E}}$ to the current. If we perform simulations in which we do not integrate over the variable $\mathbf{E}_g$ we find a summation of the Coulomb energy which is *different from* that generally used in the Ewald method, but identical to that implied when integrating the Maxwell equations.

A. Implementation

The system is discretized by placing charged particles on the $N = L^3$ vertices of a periodic cubic lattice, $\{i\}$. The components of the electric field $E_{i,j}$ are associated with the $3N$ links $\{i,j\}$ of the lattice. There are $3N$ plaquettes on the lattice each defined by four links. We use the notation $E_{1,2}$ to denote a local contribution to electric flux leaving 1 towards 2. If the link from i to j is in the positive x direction we consider that this is the local value of the x component of the field $\mathbf{E}$. The $3N$ variables $E_{i,j}$ are thus grouped into N three-dimensional vectors.

It is convenient to consider Gauss' law in the equivalent integral form

$$\int \mathbf{E}\cdot d\mathbf{S} = e_i/\epsilon_0, \tag{23}$$

where e_i is the total charge at the site i, enclosed by the surface integral, which we discretize as

$$\Lambda^2\sum_j E_{i,j} = e_i/\epsilon_0. \tag{24}$$

Λ is the lattice spacing. The sum in Eq. (24) corresponds to the total electric flux leaving the site i through the surrounding plaquettes. Since we are considering $E_{i,j}$ as a directed flux we have $E_{i,j} = -E_{j,i}$.

In order to integrate over $\overline{\mathbf{E}}$ we add a global background vector $\mathbf{E}_g$ to $E_{i,j}$. The background field does not contribute to the divergence of the electric field, it does, however contribute to the energy

$$\mathcal{U}=\frac{\Lambda^3\epsilon_0}{2}\sum_{\text{links}}(E_{i,j}+E_g^{\alpha})^2, \tag{25}$$

with E_g^{α} the component of the background field parallel to the link i,j. For convenience we also store the sum of the variables $E_{i,j}$, we denote this single 3-vector $\mathbf{E}_{\text{total}}$. For instance the x component, $E^x_{\text{total}}=\Sigma_x E_{i,j}$, where the sum is over all x directed links. We note that $\overline{\mathbf{E}}=\mathbf{E}_{\text{total}}/N+\mathbf{E}_g$.

With this discretization of the electric field we check the derivation of the Coulomb interaction between charged particles. Particles now interact via a lattice Green function, rather than with the continuum Green function of $G_c=1/r$: The interaction is identical to that found from solving the Poisson equation with a simple difference scheme on the same lattice. Explicitly we find that

$$G_l=\int\frac{d^3\mathbf{q}}{(2\pi)^3}\frac{e^{i\mathbf{q}\cdot\mathbf{r}}}{6-2\cos q_x-2\cos q_y-2\cos q_z}. \tag{26}$$

The lattice also regularizes the self energy of the particles which scales as $e_i^2/\epsilon\Lambda$. This self-energy is analogous to the Born self-energy important in solvation theory.

B. Particle motion

The simulation starts with Gauss' law satisfied as an initial condition. We displace a charge, e situated on the lattice site, 1, to the neighboring site, 2; for figures and more detail we refer the reader to our previous work.[8] The constraint is again satisfied after motion of the particle if the field associated with the connecting link is updated according to the rule $E_{1,2}\rightarrow E_{1,2}-e/\epsilon_0\Lambda^2$. The trial is accepted or rejected according to the Metropolis algorithm. If the move is accepted we must remember to modify $\mathbf{E}_{\text{total}}$. It is this update that leads to the slaving of $\overline{\mathbf{E}}$ to the current, Eq. (13), since it corresponds to $\epsilon_0\dot{\mathbf{E}}=-\mathbf{J}$

C. Plaquettes

We integrate over all transverse modes in the partition Eq. (7) by modifying together the four link field values of one of the $3N$ plaquettes. In such an update the sum of the entering and leaving fluxes at each site does not change. This update modifies the electric field by a pure circulation; $\mathbf{E}_{\text{total}}$ does not change. We perform this update by choosing one of the $3L^3$ plaquettes randomly. The amplitude of the trial update is uniformly distributed between $-\theta_0$ and θ_0, where θ_0 is chosen to have an acceptance rate of between 40% and 60%.

Let us note that the distinction between link and plaquette degrees of freedom is very similar to that found in the Yee algorithm for integrating Maxwell's equations.[12]

D. Background field

The Metropolis algorithm for the variable $\mathbf{E}_g$ is assured by using the energy Eq. (25). However, since the individual link fields, E_{ij}, are unchanged when we modify $\mathbf{E}_g$ we calculate the *change* in energy using the simplified expression

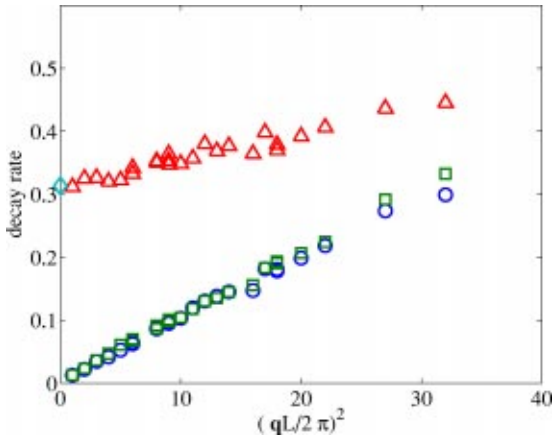

FIG. 1. Decay rate, in particle-sweeps, of correlation functions as a function of wave vector. □, density fluctuations; △, charge fluctuations; ○, transverse electric field. 60 000 particle-sweeps, 8 recordings per sweep. $\Lambda=1$, temperature $T=0.5$, $|e|=1$, $\gamma=1/2$, $\epsilon=1$. The single mode at $\mathbf{q}=0$ describes the dynamics of $\overline{\mathbf{E}}$.

$$\mathcal{U}_g=\frac{\Lambda^3\epsilon_0}{2}(N\mathbf{E}_g^2+2\mathbf{E}_g\cdot\mathbf{E}_{\text{total}}). \tag{27}$$

By following the evolution of $\mathbf{E}_{\text{total}}$ we avoid having to calculate the sum of the electric fields; modification of the global field is possible in a time which is O(1).

VI. EFFICIENCY

In Ref. 10 we gave a demonstration of the efficiency of the algorithm for a charged lattice gas; in this section we hope to convince the reader that the algorithm is equally efficient in simulating dipolar systems in the absence of Debye screening.

To model a dipolar system we take a lattice gas of charged (and self-avoiding) particles as described above and pair each positive charge with a negative charge: They are linked by a harmonic, zero length, spring so that the elastic energy between them is given by $\mathcal{U}_{\text{spring}}=\gamma(\mathbf{r}_i-\mathbf{r}_j)^2/2$, $\mathbf{r}_i$ is the position of the particle i on the lattice, γ the spring stiffness. During the simulation we record the Fourier components of several important quantities: the charge density, the particle density and the transverse electric field [that part of the field for which the discrete divergence Eq. (24) is zero]. From these recordings we deduce the two-time correlation functions. We find that the temporal correlations of the Fourier components are well described by single exponentials, as described previously.[10]

We now plot the decay rate of each mode measured in "particle-sweeps" as a function of the wave vector, Fig. 1. One particle-sweep is defined as the time needed to attempt (on average) one update for each *particle* in the simulation, independent of the number of Monte Carlo trials on other degrees of freedom; we update the plaquettes with various rates in order to study the effect on the dynamics. Measuring time in this way allows us to study the intrinsic dynamics of the dimers and their coupling to the transverse field. Note that the computational effort needed to move a particle or to update a plaquette is almost the same; both are dominated by

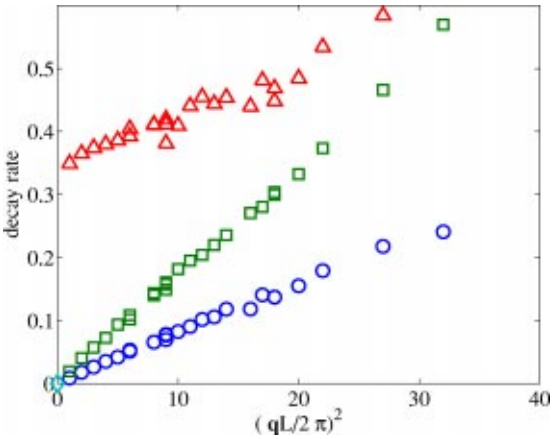

FIG. 2. As Fig. 1 but with charge-free dimers. Charge correlation function replaced by partial structure factor sensitive to internal dimer motion. The dimers are diffusing faster.

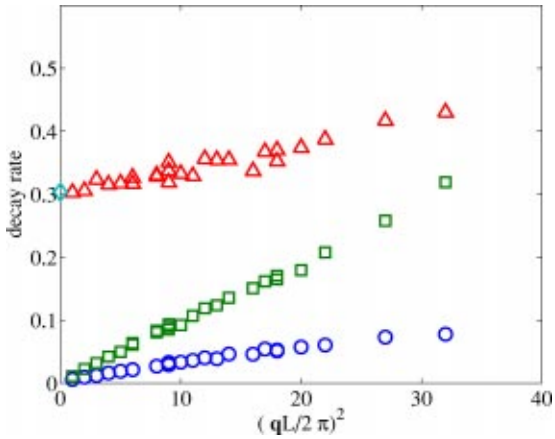

FIG. 3. As Fig. 1 but with fewer updates to transverse modes. Dimers carrying charges. The relaxation dynamics of density fluctuations and the charge fluctuations are only slightly modified despite the order of magnitude decrease in the work done on the plaquettes.

the time needed to generate random numbers and calculate the exponential function needed for the Metropolis algorithm. In our simulations we used a lattice of $L^3=20^3$ sites and 24 000 plaquettes with 1200 dimers (2400 particles).

In looking at Fig. 1 one should first note that there are two diffusive modes, with the decay rate proportional to $\mathbf{q}^2$, where $\mathbf{q}$ is the wave vector of the mode. They correspond to density fluctuations and to electric field diffusion, described by Eq. (20). The third mode, describing charge fluctuations, has a finite frequency at long wavelengths; it couples to the internal modes of the dimers which relax rapidly due to the spring.

For illustrative purposes we have tuned the relative probabilities of particle motion and plaquette updates in Fig. 1 so that the diffusion rates of the density and the transverse electric field are very similar. To do this we used a relative probability (per degree of freedom) of particle motion to plaquette updates of 1: 1/3. Since there are considerably more plaquettes than particles about 75% of the time in the simulation is devoted to updating the transverse field. For simplicity we do not update $\mathbf{E}_g$; we are simulating with ''Maxwell'' boundary conditions.

In Fig. 2 we simulate a similar system with the same ratio of particle motion to plaquette updates. The only modification is that the charges on the dimers are now put to zero; there is no charge in the simulation. We note two points in comparison with Fig. 1. The diffusion rate of the dimers has increased by some 60%, while the diffusion rate of the electric field has slightly fallen. In this plot we replace the charge–charge correlation function by an analogous partial structure factor, in which the scattering amplitude of one particle in a dimer is $+1$, while the second particle has a scattering amplitude of -1. This structure factor is again sensitive to the internal dynamics of the dimer.

In Fig. 3 we again simulate charged dimers, we reduce however the number of plaquette updates in the simulation so that they now occur in the relation 1: 1/30. In this simulation 75% of the time is spent updating the position of the particles, only 25% of CPU time is devoted to the transverse field. As might be expected the propagation of the transverse modes has slowed down. However the equilibration of the charge and density modes is not greatly modified in comparison with Fig. 1.

In Fig. 4 we have simulated charge-free dimers with plaquettes updated in the proportion of 1: 1/30. We note that compared with Fig. 3 (where the dimers carry charges) the transverse modes have substantially slowed. Motion of the particles is playing an important role in agitating the field variables in Fig. 3; this accelerates the propagation of the electric field.

From our results on the simulation on this simple dimer system we find that quite remarkably one can ''get away'' with very little work on the plaquette degrees of freedom. How can this be so? Motion of a particle along the four links defining a plaquette is equivalent to a single plaquette update; the motion of the particles is, on its own, quite good at integrating over the transverse degrees of freedom. This integration is clearly imperfect since the only values of the plaquette circulation that are generated are integral multiples of $e/\epsilon\Lambda$. We see, however, that the plaquette updates only

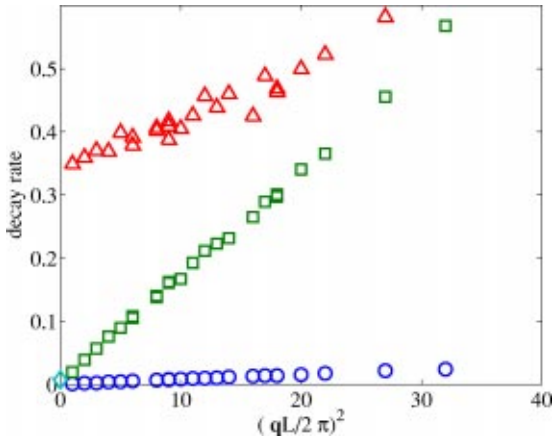

FIG. 4. As Fig. 1 but with fewer updates to transverse modes and charge-free dimers. The dynamics of the transverse modes have slowed in comparison with Fig. 3 in the absence of coupling to the charges.

have to "fill in" between the integral multiples of $e/\epsilon\Lambda$ rather than perform the full integration of these modes.

It is also rather natural that longitudinal and transverse modes (with scalar and vector symmetries) are *weakly coupled* in a homogeneous system at long wavelengths; the lowest order couplings occurring in the free energy are presumably at least cubic; if the number density fluctuation is n and the transverse field fluctuation $\mathbf{e}_{\mathrm{tr}}$ one could expect that the lowest order coupling in a Landau picture is $\mathbf{e}_{\mathrm{tr}}^2 n$.

Examining the figures we see that the total overhead in simulating the charged dipole, compared to a charge-free dimer is about a factor 2 with appropriately chosen simulation parameters.

The simulation of Fig. 1 corresponds to 30 min of simulation on a pentium 4 2.5 GHz. Total clock time was (much) longer due to the overhead of the Fourier analysis of the mode structure.

We note that the temperatures used in these simulations is *very* high compared with those of interest in condensed matter physics. The Bjerrum length is comparable to the particle size in these simulations at a temperature of about $T=1/4\pi$, the present simulations are however at $T=1/2$. We find that at low temperatures the mobility of the particles drops very strongly, since there is a finite barrier for particle motion due to the discrete nature of the charges and the lattice. We have recently implemented an off lattice version of the algorithm and find that we can easily overcome this artifact of the discretization.[13]

VII. POISSON–BOLTZMANN SIMULATIONS

Classic methods for treating the Poisson–Boltzmann equation require a calculation of the long ranged Coulomb interaction, either in real space or in Fourier space.[14] In this section we show how constrained Monte Carlo gives rise to a local treatment of the Poisson–Boltzmann equation. The method, however, has some original features since rather than considering the minimum of the Poisson–Boltzmann functional we integrate over the charge degrees of freedom, creating a fluctuation enhanced Poisson–Boltzmann algorithm.[15]

A. Formulation of the free energy

Consider a system of n particles in a fixed volume V with coordinates $\mathbf{q}$. The partition function is

$$\mathcal{Z}=\int e^{-\beta\mathcal{U}}d\mathbf{q}, \tag{28}$$

where $\mathcal{U}$ is the configurational contribution to the energy and the integral is over all particle positions. Let us coarse grain the evaluation of the partition function by subdividing the volume V in to a large number of elementary cells of volume Λ^3, replacing the configuration integrals by sums. In each cell let there be n_i particles. Then

$$\mathcal{Z}=\sum n!\prod_i \left(\frac{\Lambda^{3n_i}}{n_i!}\right)e^{-\beta\bar{\mathcal{U}}}. \tag{29}$$

Here the combinatorial factor counts the number of ways of distributing particles between boxes and the energy has been re-expressed in a coarse grained manner, $\mathcal{U}=\bar{\mathcal{U}}(n_i)$, in terms of the cell occupation numbers. The factor Λ^{3n_i} comes from the n_i fold integral over the cell volume. Re-expressing the n_i in terms of local concentrations of particles, $\rho_i=n_i/\Lambda^3$, and exponentiating the combinatorial factor [using $\log(n!)\approx n\log n-n$] we find the effective energy function for the coarse grained description

$$\mathcal{H}=k_BT\Lambda^3\sum_i(\rho_i\ln(\rho_i\Lambda^3)-\rho_i)+\bar{\mathcal{U}}(\{\rho_i\}), \tag{30}$$

where the sum over i is now a sum over both boxes and chemical species. This expression is very similar to that used in many mean field studies, but the derivation shows that this effective energy function is valid for *fluctuating* densities. It is *not* a functional simply valid as a minimum principle as is emphasized in density functional approaches to the Poisson–Boltzmann equation. In our simulations the variables ρ_i are fluctuating variables.

In order to describe a charged coarse grained fluid we must choose Λ: The ions are separated on average by a distance $\xi=\rho^{-1/3}$ while the Bjerrum length is given by $\ell_b=e^2/4\pi k_BT\epsilon$. We also introduce a further length scale: the Debye length, the length scale at which the energy stored in the electric field, due to concentration fluctuations, is equal to k_BT; we find that $\ell_d^2\sim\xi^3/\ell_b$. In order to use the coarse grained entropy we require that $\Lambda\gg\xi$ so that $n_i\gg1$, however if we wish to describe screening in detail we also require $\Lambda\ll\ell_d$ implying a relatively narrow window of possible values for the coarse graining parameter.

The full system we simulate is

$$\mathcal{H}=k_BT\Lambda^3\sum_i(\rho_i\ln\rho_i\Lambda^3-\rho_i)+\frac{\Lambda^3}{2}\epsilon_0\sum_{\mathrm{links}}E_{i,j}^2, \tag{31}$$

where the electric field is constrained by Gauss' law, with both external charges and ρ_i acting as sources.

Other contributions to the free energy varying in $\rho^{3/2}$ are often introduced as local field corrections in density functional theories. However, such energies are derived on a length scale larger than the Debye length and are due to correlations of the electric field over ℓ_d. In the effective free energy measured on a scale $\Lambda<\ell_d$ such terms should not be added by hand. They will be generated automatically by the algorithm via fluctuations in the charges.

The derivation of the effective Hamiltonian on the scale Λ is rather close in spirit to the renormalization group. It would be interesting to perform the numerical renormalization group on a charged fluid in order explicitly measure the effective Hamiltonian as a function of the scale for $\xi<\Lambda<\ell_d$. The derivation breaks down in some particularly interesting cases, including strongly charged surfaces. In this case a new, independent, length, the Gouy–Chapman length becomes smaller than the coarse graining cell.

As a test of the algorithm we simulated, Fig. 5, a uniform positively charged plane in a background of positive and negative ions. We see the depletion of the positive ions and the attraction of negative ions near the surface. In the simulation the plane was stationary however the method allows parallel dynamics of both the ionic and the macro-ion

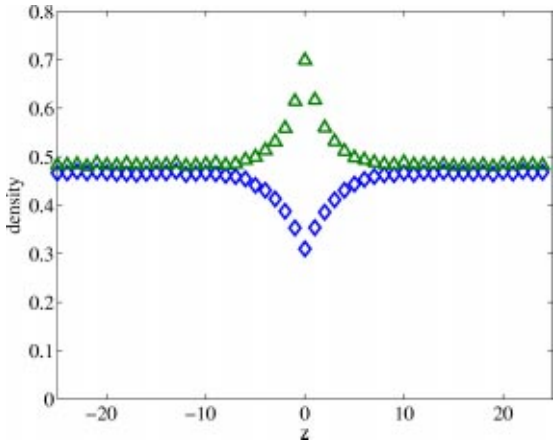

FIG. 5. A positively charged plane is simulated in the presence of counterions using the Poisson-Boltzmann formulation Eq. (31). We plot the concentration of the two, symmetric ion concentrations as a function of the distance from the plane. System of size $50\times50\times50$. Concentration is for a single equilibrated system. △ negative charges, ◇ positive charges.

degrees of freedom without having to perform global updates or optimizations. Such simulations are useful in the simulation of flexible charged objects such as polyelectrolytes within the Poisson–Boltzmann approximation; in such flexible objects we can individually update the position of individual charges in the macro-ion as described in the application to electrolytes. The method is less likely to be useful in the simulation of large rigid objects such as a colloidal sphere carrying large charges. In such cases the simultaneous modification of **E** on many links leads to a low Monte Carlo acceptance rate, or when working off-lattice small step sizes. Our method is also incompatible with smart global algorithms, such as the pivot algorithm in polymer simulation, for similar reasons.

In the functional Eq. (31) we integrate over the continuous variables ρ_i. However, numerically it is just as easy to keep the discrete charges, n_i. In such a way one still describes a coarse grained system so that $\langle n_i\rangle>1$ but a higher degree of detail is retained. A improved account for the entropy is also possible if a better approximation for $\log(n!)$ is used. It would be particularly interesting to understand if attractive, correlation effects can be reproduced within such a coarse grained, discrete model.

Finally we wish to make some remarks about the ergodicity of the Poisson–Boltzmann algorithm: We have already seen in our dipolar model that the motion of the charges excites transverse degrees of freedom of the field. It was only the discreet nature of the charges in the dipolar system which prevented the transverse field from coming to equilibrium even in the absence of independent field updates. In the Poisson–Boltzmann algorithm the amount of charge transfered at each step is randomly chosen: the algorithm is ergodic *even without the field updates* which can be dropped from the algorithm.

B. Screened Coulomb interactions

In even coarser-grained treatments of charged systems the counterion degrees of freedom are eliminated entirely by using an effective Yukawa interaction $e_1e_2\exp(-\kappa r)/r$. One implements this potential numerically by introducing a *nonconstrained* energy function for the electric field:

$$\mathcal{U}_Y=\frac{\epsilon_0}{2}\int[\mathbf{E}^2+\kappa^{-2}(\operatorname{div}\mathbf{E}-\rho/\epsilon_0)^2]\mathrm{d}^3\mathbf{r}. \tag{32}$$

The analytic treatment of this energy is simpler than the constrained functions that we have considered until now; the functional is Gaussian in the field **E**. Clearly the limit $\kappa\to0$ leads to a constrained electric field. Taking the functional derivative of Eq. (32) with respect to the electric field we find

$$\kappa^2\mathbf{E}-\operatorname{grad}\operatorname{div}\mathbf{E}=-\operatorname{grad}\rho/\epsilon_0 \tag{33}$$

for the stationary points of the energy function. This equation is best treated by separating the transverse and longitudinal components of **E**. The longitudinal component of the electric field gives rise to the Yukawa potential at the minimum of Eq. (32). The transverse components of **E** do not couple to the density.

When κ is small the screening length becomes large and the field becomes more and more constrained by Gauss' law. Freely chosen Monte Carlo moves with Eq. (32) then become inefficient since small amplitude trials are needed. It becomes more efficient to separate the Monte Carlo moves into two classes, those which conserve $\operatorname{div}\mathbf{E}-\rho/\epsilon_0$ and those which modify it.

VIII. OFF-LATTICE INTERPOLATION AND RELATION TO PLASMA SIMULATIONS

We now formulate the algorithm when the particles are moving in the continuum but with charges interpolated to the cubic grid. We shall see that the simplest generalization of our method is closely related to numerical methods used in plasma simulation.

Consider a single particle within a cell of the grid. We here take $\Lambda=1$ and consider a cube such that $0<\{x,y,z\}<1$. The simplest interpolation of the charges to the lattice is a linear interpolation so that the charge at the site (0,0,0) is equal to $e(1-x)(1-y)(1-z)$. Interpolating to the eight sites of the enclosing cube preserves both the total charge and the dipole moment.

When the particle moves the rate of change of the density at the origin is

$$F(t)=-e[(1-x)(1-y)\dot z+(1-x)(1-z)\dot y+(1-y)(1-z)\dot x]. \tag{34}$$

This variation has a simple, direct interpretation as currents in the links:

$$J_z=e(1-x)(1-y)\dot z \tag{35}$$

is the current in the z direction on the link between (0,0,0) and (0,0,1).

Equation (34) is a perfect differential so that when the particle is transported around a loop

$$\int F(t)dt=0, \tag{36}$$

implying that the interpolated charge returns to its initial value; this is a clearly needed consistency requirement for the current.

Consider now Monte Carlo: We need to generalize the expression for J_z to finite displacements, while preserving Eq. (36). Take a path that starts at (x_i,y_i,z_i) and finishes at $(x_{i+1},y_{i+1},z_{i+1})$ after a time $t=1$. We integrate the expression, Eq. (35) for the link current to find

$$\begin{aligned}\Delta e_z/e &= \int_0^1 (1-x_i-v_x t)(1-y_i-v_y t)v_z \mathrm{d}t \\ &= (1-x_i)(1-y_i)v_z \\ &\quad - \frac{(v_x(1-y_i)+v_y(1-x_i))v_z}{2} + \frac{v_x v_y v_z}{3}, \end{aligned} \tag{37}$$

where $v_x = x_{i+1} - x_i$. By construction a series of such steps satisfies an expression equivalent to Eq. (36). The transfered charge Δe_z leads to a corresponding modification of the electric field on the link $E \to E - \Delta e_z/\epsilon_0$.

While being a low order interpolation scheme Villasenor and Buneman[16] showed that such a Gauss' law conserving scheme allows long time, stable integration of plasma equations. Many other (nonconserving) methods need a periodic correction step in which Poisson's equation is solved to reinitialize the longitudinal electric field, leading to complicated and slow code. We again see the central role played by Gauss' law in the efficient simulation of charged systems; codes based on Buneman's TRISTAN would seem to be the closest analogy in the literature to our algorithm.

For the simplest, low precision modeling of polymers and polyelectrolytes we expect that this present scheme will already be useful. The scheme needs to be improved by interpolation over several cells in order to be competitive in accuracy with those that are currently used in the soft condensed matter simulation community.[2] We present one possible algorithm in an accompanying paper[13] on charge and current interpolation.

IX. INHOMOGENEOUS MEDIA

The forces on charges in the presence of inhomogeneous dielectric media are complicated; a charge is attracted towards regions of high ϵ. Such forces are well known to be important in the structuring of charge distribution around proteins[17] and at surfaces.

The electric energy of an arbitrary inhomogeneous medium is given[18] by

$$\mathcal{U} = \int d^3\mathbf{r} \frac{\mathbf{D}^2}{2\epsilon(\mathbf{r})}, \tag{38}$$

where the electric displacement, $\mathbf{D} = \epsilon(\mathbf{r})\mathbf{E}$, obeys the constraint $\mathrm{div}\,\mathbf{D} = \rho$. The generalized Poisson equation found from this constrained variational problem is

$$\mathrm{div}(\epsilon(\mathbf{r})\mathrm{grad}\,\phi) = -\rho, \tag{39}$$

so that the electrostatic energy is given by

$$\mathcal{U}_{\mathrm{elec}} = \int d^3\mathbf{r} \frac{\epsilon(\mathbf{r})}{2} (\mathrm{grad}\,\phi_p)^2. \tag{40}$$

The solution to the constraint equation in nonperiodic media is

$$\mathbf{D} = -\epsilon(\mathbf{r})\mathrm{grad}\,\phi + \mathrm{curl}\,\mathbf{Q}. \tag{41}$$

As for the case of homogeneous media the energy Eq. (38) can be written as a sum of two terms corresponding to electrostatic and fluctuation contributions.

The statistical mechanical treatment of inhomogeneous dielectric media is however more complicated than the case of homogeneous systems: We have seen that when ϵ is a constant the contribution of the transverse fluctuations to the free energy is independent of the positions of the particles; the algorithm gives rise to pure Coulomb interactions between particles. Here we shall show that in addition to the electrostatic interactions, Eq. (40), we also generate extra dipole–dipole interactions.

We shall show that the fluctuation potentials are expected on general grounds in inhomogeneous media, they correspond to the Keesom potential[19] varying as $1/r^6$ between fluctuating permanent dipoles. These interactions should be distinguished from the van der Waals interaction (also in $1/r^6$) which has its origins in quantum mechanics.[21]

A. Dipolar forces

In this section we consider the fluctuation potentials in the absence of charges, then

$$\mathcal{Z} = \int \mathcal{D}\mathbf{D} e^{-\int [\beta \mathbf{D}^2/2\epsilon(\mathbf{r})]\mathrm{d}^3\mathbf{r}} \prod_{\mathbf{r}} \delta(\mathrm{div}\,\mathbf{D}(\mathbf{r})). \tag{42}$$

This energy is a function of the position of the particles due to the presence of $\epsilon(\mathbf{r})$ in the denominator of the energy.

We will proceed by first rewriting the constrained field $\mathbf{D}$ in terms of a projection operator. This is easily done in Fourier space where one can trivially separate longitudinal and transverse components of a vector field. We then perform an inverse Fourier transform to find the analytic form of the projection operator in real space. Rather surprisingly we find that this projection operator is closely related to dipolar interactions which vary in $1/r^3$. An expansion to second order in the fluctuations in the dielectric constant then gives a contribution to the free energy which naturally decreases as $1/r^6$.

One calculates a transverse field from a general unconstrained field $\mathbf{D}$ by subtracting off the longitudinal component:

$$\mathbf{D}_t(\mathbf{q}) = \mathbf{D}(\mathbf{q}) - \frac{\mathbf{q}(\mathbf{q}.\mathbf{D}(\mathbf{q}))}{q^2}. \tag{43}$$

Since we extract the transverse component by multiplication in Fourier space the same operation can be written as a convolution in real space:

$$\mathbf{D}_t(\mathbf{r}) = \int d^3\mathbf{r}_1 \mathcal{T}(\mathbf{r},\mathbf{r}_1)\mathbf{D}(\mathbf{r}_1) \tag{44}$$

with a real space projection operator $\mathcal{T}$. This inverse Fourier transform is a little tricky to perform: The projection operator does not decay "nicely" for large q. We proceed more carefully using various operator identities.

We consider the function $\mathbf{v}(\mathbf{r})\cdot\mathbf{D}_t(\mathbf{r})$ for an arbitrary vector $\mathbf{v}(\mathbf{r})$. We note that $i\mathbf{q}\cdot$, $i\mathbf{q}$ and $1/q^2$ are respectively the Fourier transforms of div, grad, and $1/4\pi r$. This results in

$$\mathbf{v}(1)\cdot\mathbf{D}_t(1)=\int \mathbf{v}(1)\left(\delta(1,2)+\frac{1}{4\pi r_{12}}\,\mathrm{grad}\,\mathrm{div}\,\mathbf{D}(2)\right)d2. \tag{45}$$

We have used a common shorthand notation replacing $\mathbf{r}_i$ by the index i. We now integrate by parts twice (using the fact that the operators div and $-$grad are mutually adjoint) to transfer the derivatives from $\mathbf{D}$ to $\mathbf{v}/r$ while discarding surface terms:

$$\mathbf{v}(1)\cdot\mathbf{D}_t(1)=\int \mathbf{D}(2)\left(\delta(1,2)+\mathrm{grad}\,\mathrm{div}\frac{1}{4\pi r_{12}}\right)\mathbf{v}(1)d2. \tag{46}$$

The operators "grad" and "div" act on the "2" degrees of freedom so that $\mathbf{v}(1)$ is to be considered as a constant. One simplifies using the identity

$$\mathrm{grad}(\mathbf{v}\cdot\mathrm{grad}(1/r))=(\mathbf{v}\cdot\mathrm{grad})(\mathrm{grad}(1/r))=\frac{3(\mathbf{v}\cdot\hat{\mathbf{r}})\hat{\mathbf{r}}-\mathbf{v}}{r^3}\quad\text{for}\quad r\neq 0 \tag{47}$$

leading to

$$\mathcal{T}(\mathbf{r})=\frac{2}{3}\delta(\mathbf{r})\mathbf{I}+\frac{3|\hat{\mathbf{r}}\rangle\langle\hat{\mathbf{r}}|-\mathbf{I}}{4\pi r^3}. \tag{48}$$

$\mathbf{I}$ is the unit matrix. The coefficient of the delta function is a little subtle but is found by noting that the trace of an operator is independent of the basis: A projection operator which selects the two transverse degrees of freedom has trace two.

The transverse projector is closely related to dipolar interaction between particles. For instance the electrostatic interaction between two dipoles $\mathbf{p}_1$ and $\mathbf{p}_2$ when $\mathbf{r}_1\neq\mathbf{r}_2$ is just[22]

$$\mathcal{U}_{1,2}=-\mathbf{p}_1\mathcal{T}_{1,2}\mathbf{p}_2/\epsilon_0 \tag{49}$$

as is discussed in many standard texts.[4] $\mathcal{T}$ has the useful property

$$\int \mathcal{T}(0,1)\cdot\mathcal{T}(1,2)d^3 1=\mathcal{T}(0,2) \tag{50}$$

since it is a projection operator and thus idempotent. Here "$\cdot$" signifies matrix multiplication of the operator $\mathcal{T}$.

We now proceed by perturbation theory in fluctuations in the dielectric constant. Let us consider two small inhomogeneities in the dielectric properties separated by a large distance; the background dielectric constant is ϵ_0. One expands the partition function to second order in the perturbation. Each fluctuation in the dielectric constant has associated with it an amplitude $(1/\epsilon(\mathbf{r})-1/\epsilon_0)\approx-\delta\epsilon/\epsilon_0^2$.

The second order perturbation in the partition function due to interaction between two sites "a" and "b" is found to be

$$\Delta_2(a,b)=\frac{\beta^2}{4\epsilon_0^4}\int \delta\epsilon(a)\delta\epsilon(b)d^3\{1234\}\times\mathbf{D}(1)\mathcal{T}(1,a)\cdot\mathcal{T}(a,2)\mathbf{D}(2)\times\mathbf{D}(3)\mathcal{T}(3,b)\cdot\mathcal{T}(b,4)\mathbf{D}(4), \tag{51}$$

which needs to be averaged with the statistical weight from Eq. (42). The interesting pairings are $\langle\mathbf{D}(1)\mathbf{D}(4)\rangle\times\langle\mathbf{D}(2)\mathbf{D}(3)\rangle$ and $\langle\mathbf{D}(1)\mathbf{D}(3)\rangle\langle\mathbf{D}(2)\mathbf{D}(4)\rangle$. To perform the integration over transverse modes we introduce the modified energy functional

$$\overline{\mathcal{U}}=\int\frac{\overline{\mathbf{D}}^2}{2\epsilon_0}d^3\mathbf{r}, \tag{52}$$

$$\overline{\mathbf{D}}(\mathbf{q})=(1+\lambda|\mathbf{q}\rangle\langle\mathbf{q}|)\mathbf{D}(\mathbf{q}). \tag{53}$$

In the limit of λ large and positive all longitudinal fluctuations are suppressed in the measure, however we can now perform usual, unconstrained perturbation theory with this Gaussian energy. In the limit of large λ the appropriately normalized correlators become

$$\langle D_i(1)D_j(2)\rangle=\epsilon_0 k_B T\mathcal{T}_{i,j}(1,2). \tag{54}$$

The calculation is much simplified by making use of the identity Eq. (50). The free energy cost of dielectric inhomogeneity is given by

$$F=-k_B T\ln\mathcal{Z}=F_0+V(a,b), \tag{55}$$

where F_0 is the free energy of a uniform dielectric medium. The potential between particles is found to be

$$V(a,b)(r)=-\frac{k_B T v_a\delta\epsilon_a v_b\delta\epsilon_b}{2\epsilon_0^2}\mathrm{Tr}\,\mathcal{T}^2(a,b) \tag{56}$$

$$=-\frac{3k_B T v_a\delta\epsilon_a v_b\delta\epsilon_b}{(4\pi\epsilon_0)^2 r_{a,b}^6}, \tag{57}$$

with v_i the volume of the dielectric inhomogeneity. Substituting that the relative dielectric constant for a weakly dipolar material (with ϵ_i/ϵ_0-1 small) is given by

$$\epsilon_i/\epsilon_0=1+\frac{\mathbf{p}_i^2 n_i}{3\epsilon_0 k_B T}, \tag{58}$$

with n_i the density of dipoles of strength $\mathbf{p}_i$ we recognize the Keesom potential[19] between pairs of thermally agitated permanent dipoles

$$V_K=-\frac{\mathbf{p}_a^2\mathbf{p}_b^2}{3k_B T(4\pi\epsilon_0 r^3)^2}. \tag{59}$$

Note the distinction between free energy and internal energy for the Keesom potential. The internal energy is given by

$$u_K=\frac{\partial}{\partial\beta}\beta F. \tag{60}$$

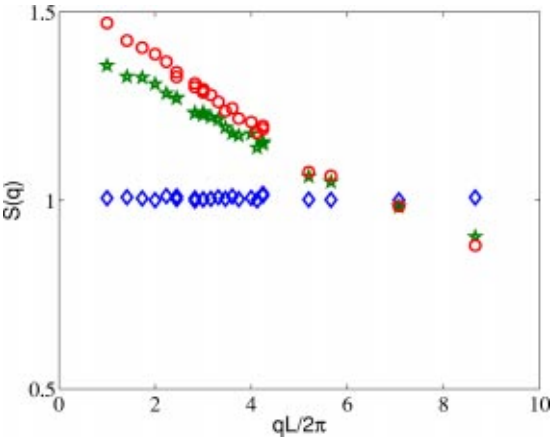

FIG. 6. Plot of the density–density structure factor as a function of the wave vector. 1000 neutral particles simulated on a $15\times15\times15$ grid. $\diamond$, $\epsilon_p=\epsilon_0$; $\star$, $\epsilon_p=5\epsilon_0$; $\bigcirc$, $\epsilon_p=0.2\epsilon_0$. For small q the structure factor increases, reflecting attractive interactions between the particles when $\epsilon_p\neq\epsilon_0$.

When the dipole moments are independent of the temperature $u_K=2V_K$. If ϵ_i is independent of the temperature $u_K=0$; the potential is purely entropic.

The presence of these dipole terms seems inevitable in the Monte Carlo algorithm: Removing them requires the evaluation of a complicated multibody determinant. The algorithm is closer in spirit to simulations which replace the dielectric medium by an ensemble of fluctuating Langevin dipoles[20] than the classic, zero temperature, solution of the Poisson equation.

B. Simulations

Let us discretize the energy Eq. (38) by placing the particles on the vertices of a cubic network. To each lattice point we also associate a dielectric constant ϵ_i. The energy associated with a link "i,j" is then defined to be

$$\mathcal{U}_{i,j}=\Lambda^3\frac{D_{i,j}^2}{4}\left(\frac{1}{\epsilon_i}+\frac{1}{\epsilon_j}\right). \tag{61}$$

The constraint $\Lambda^2\Sigma_j D_{i,j}=e_i$ is imposed as an initial condition on **D** rather than **E**. The electric displacement **D** is updated in a similar manner to that described above for the electric field. The algorithm is simple compared with direct solution of the Poisson Eq. (39); in particular we note that Fourier methods do not diagonalize the Poisson equation when ϵ is a function of the position.

We implemented the algorithm for a neutral lattice gas of dielectric constant ϵ_p embedded in a background ϵ_0 in the absence of free charges. The density–density correlation functions $S(q)$ were measured to characterize the effect of interactions, Fig. 6. As expected when $\epsilon_p=\epsilon_0$ no structure appears in the simulation. For both $\epsilon_p<\epsilon_0$ and $\epsilon_p>\epsilon_0$ the structure factor increases for small q. This can be interpreted as being due to an attractive interaction between the particles leading to clumpiness in the structure.

C. Low symmetry materials

In low symmetry materials the dielectric constant is a tensor, with up to three distinct eigenvalues and eigenvectors. The algorithm generalizes to this case; in such materials the constraint equation is

$$\operatorname{div}\mathbf{D}=\rho, \tag{62}$$

where $\mathbf{D}=\boldsymbol{\epsilon}\mathbf{E}$; $\boldsymbol{\epsilon}$ is a matrix to that **D** and **E** need no longer be parallel. The electric energy

$$\mathcal{U}=\tfrac{1}{2}\int \mathbf{D}\boldsymbol{\epsilon}^{-1}\mathbf{D}\mathrm{d}^3\mathbf{r}. \tag{63}$$

$\boldsymbol{\epsilon}^{-1}$ denotes the matrix inverse.

One possible application of this discretization is in liquid crystals where the order parameter manifests itself as a dielectric anisotropy. Models are easily constructed within a mean field description. This permits numerical study of transitions driven by electric fields.

X. CONCLUSIONS

This paper has presented local algorithms for the simulation of charged systems. Our methods are strongly inspired by the observation that Maxwell's equations allow a local evolution of field degrees of freedom leading to the Coulomb interaction. It introduced dynamics which conserve $\operatorname{div}\mathbf{E}-\rho/\epsilon$ while starting the simulation with this constraint satisfied. The Monte Carlo algorithm eliminates the magnetic degrees of freedom from Maxwell's equations leading to pure electrostatic interactions.

The method is rather general and can be used in many situations: for instance application of the constrained formalism to path integral Monte Carlo should be equally straight forward as the cases treated here. The main weaknesses that we see in the algorithm are

(1) Incompatibility of constraint preservation with simulations in the grand-canonical ensemble, so useful in the study of phase behavior.
(2) Low efficiency with large strongly charged objects undergoing coherent motion, either due to rigidity or the use of smart global moves.

The code used in the simulations is available from the author.

ACKNOWLEDGMENT

I would like to thank Ralf Everaers for many discussions, essential in the formulation of these algorithms.

[1] L. Greengard and V. Rokhlin, J. Comput. Phys. **73**, 325 (1987).
[2] E. Essmann, L. Perera, M. L. Berkowitz, T. Darden, H. Lee, and L. G. Pedersen, J. Chem. Phys. **103**, 8577 (1995).
[3] T. Schlick, R. D. Skeel, A. T. Brunger, L. V. Kalé, J. A. Board Jr., J. Hermans, and K. Schulten, J. Comput. Phys. **151**, 9 (1998).
[4] J. D. Jackson, *Classical Electrodynamics* (Wiley, New York, 1999).
[5] R. Feynman, *Lectures on Physics* (Addison-Wesley, Reading, 1989), Vol. 2, Chap. 19.
[6] R. Allen, J.-P. Hansen, and S. Melchionna, Phys. Chem. Chem. Phys. **3**, 4177 (2001).
[7] R. Feynman, *Lectures on Gravitation* (Addison-Wesley, Reading, 1995), Chap. 3.
[8] A. C. Maggs and V. Rossetto, Phys. Rev. Lett. **88**, 196402 (2002).

[9] S. W. de Leeuw, J. W. Perram, and E. R. Smith, Proc. R. Soc. London, Ser. A **373**, 26 (1980).
[10] A. C. Maggs, J. Chem. Phys. **117**, 1975 (2002).
[11] D. Vanderbilt, J. Phys. Chem. Solids **61**, 147 (2000).
[12] K. S. Yee, IEEE Trans. Antennas Propag. **14**, 302 (1966).
[13] J. Rottler and A. C. Maggs, J. Chem. Phys. **120**, 3119 (2004), following paper.
[14] H. Löwen, P. A. Madden, and J.-P. Hansen, Phys. Rev. Lett. **68**, 1081 (1992).
[15] R. R. Netz and H. Orland, Europhys. Lett. **45**, 726 (1999).
[16] J. Villasenor and O. Buneman, Comput. Phys. Commun. **69**, 306 (1992).
[17] M. F. Perutz, Science **206**, 1187 (1979).
[18] L. D. Landau and E. M. Lifshitz, *Electrodynamics* (Butterworth–Heinemann, London, 1999).
[19] J. Israelachvili, *Intermolecular and Surface Forces* (Academic, London, 1991).
[20] A. Warshel and M. Levitt, J. Mol. Biol. **103**, 227 (1976).
[21] We also note that unlike van der Waals interactions the Keesom potential in the presence of free charges is screened over a distance of one half of the Debye length.
[22] One oddity is that $\mathcal{T}$ is the magnetic dipole operator not the electric dipole operator (Ref. 4); they differ in the coefficient of the δ-function.